Development of realistic high-resolution whole-body voxel models of Japanese adult males and females of average height and weight, and application of models to radio-frequency electromagnetic-field dosimetry

To cite this article: Tomoaki Nagaoka *et al* 2003 *Phys. Med. Biol.* **49** 1

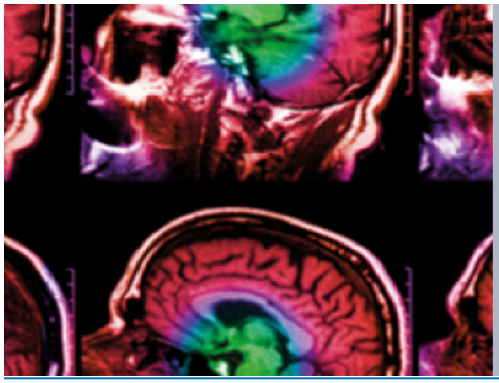

INSTITUTE OF PHYSICS PUBLISHING PHYSICS IN MEDICINE AND BIOLOGY

Phys. Med. Biol. **49** (2004) 1–15 PII: S0031-9155(04)65569-2

Development of realistic high-resolution whole-body voxel models of Japanese adult males and females of average height and weight, and application of models to radio-frequency electromagnetic-field dosimetry

Tomoaki Nagaoka[1], Soichi Watanabe[2], Kiyoko Sakurai[1], Etsuo Kunieda[3], Satoshi Watanabe[1], Masao Taki[4] and Yukio Yamanaka[2]

[1] Department of Medical Engineering, Kitasato University Graduate School of Medical Sciences, 1-15-1 Kitasato, Sagamihara, Kanagawa 228-8555, Japan
[2] Electromagnetic Compatibility Group, Communications Research Laboratory, Independent Administrative Institution, 4-2-1 Nukuikitamachi, Koganei, Tokyo 184-8795, Japan
[3] Department of Radiology, School of Medicine, Keio University, 35 Shinanomachi, Shinjuku, Tokyo 160-8582, Japan
[4] Department of Electrical Engineering, Graduate School of Engineering, Tokyo Metropolitan University, 1-1 Minami-Osawa, Hachioji, Tokyo 192-0397, Japan

E-mail: nagaoka@rtpc2.ahs.kitasato-u.ac.jp

Received 2 July 2003, in final form 6 November 2003
Published 15 December 2003
Online at stacks.iop.org/PMB/49/1 (DOI: 10.1088/0031-9155/49/1/001)

Abstract

With advances in computer performance, the use of high-resolution voxel models of the entire human body has become more frequent in numerical dosimetries of electromagnetic waves. Using magnetic resonance imaging, we have developed realistic high-resolution whole-body voxel models for Japanese adult males and females of average height and weight. The developed models consist of cubic voxels of 2 mm on each side; the models are segmented into 51 anatomic regions. The adult female model is the first of its kind in the world and both are the first Asian voxel models (representing average Japanese) that enable numerical evaluation of electromagnetic dosimetry at high frequencies of up to 3 GHz. In this paper, we will also describe the basic SAR characteristics of the developed models for the VHF/UHF bands, calculated using the finite-difference time-domain method.

1. Introduction

There is growing interest in the safety of radio-frequency (RF) electromagnetic fields (EMFs) of wireless telecommunication devices such as cellular phones. Safety of such RF-EMFs is evaluated based on specific absorption rates (SARs). The SAR in a human body exposed to a RF-EMF is, however, very difficult to measure directly because the SAR includes the internal

electric-field strength and conductivity in the body. Therefore, the SAR has been estimated by numerical methods using human-body voxel models. The SAR in the human head during cellular-phone use has recently been estimated using the finite-difference time-domain (FDTD) method and realistic voxel models of the head (Dimbylow 1994, Okoniewski and Stuchly 1996, Gandhi *et al* 1996, Watanabe *et al* 1996, Wang and Fujiwara 2000). However, we can anticipate that in the near future, a variety of wireless information terminals will be used not only in the proximity of the head, as with cellular phones, but also in the proximity of other parts of the human body. In other words, these devices will be 'worn' at different positions on the body. The evaluation of the SAR in a human body wearing such terminal devices is therefore required. However, head models alone will no longer be adequate for evaluating the SAR in areas of the body in the proximity of these devices.

Furthermore, terrestrial digital television broadcasting services have recently begun operations, with service areas slated to expand in the future. Such broadcasting requires additional broadcast towers operating in the very-high-frequency (VHF) and ultra-high-frequency (UHF) bands, and these facilities may cause public concern over the health effects of such operations. In particular, whole-body resonance in the VHF band is known to be one of the most significant factors characterizing energy absorption in the human body at these frequency bands (Gandhi 1987). However, detailed SAR characteristics for human bodies exposed to such RF-EMFs remain to be elucidated, as few whole-body human models are available to date.

Recently, progress in medical imaging technology and computer performance has enabled us to develop whole-body voxel models and to evaluate the SAR for an entire body. Dimbylow (1995) developed an anatomically realistic voxel model of an entire body to simulate reference man (170 cm, 70 kg) described in ICRP 23 (1975). This model, based on magnetic resonance imaging (MRI) data of an adult male, was named NORMAN (normalized man), and was segmented into 37 different tissue types. The resolution of NORMAN is $2.04 \times 2.04 \times 1.95$ mm^3. Gandhi and Furse (1995) developed a whole-body model with $2 \times 2 \times 3$ mm^3 resolution using MRI data of an adult male. This model was segmented into 30 different tissue types. The weight of the subject for the model was 64 kg. Therefore, the weight of their model was scaled up to approximately the weight of reference man in ICRP 23, and became about 71 kg. Zubal *et al* (1995) constructed a model torso and head using CT images of an adult male. This model consisted of $4 \times 4 \times 4$ mm^3 voxels and 68 different tissue types. Dawson *et al* (1997) created a whole-body model using the combined torso and head data reported by Zubal *et al* (1995), and leg and arm data from the visible human project (VHP) dataset at the US National Library of Medicine (http://www.nlm.nih.gov/research/visible/visible_human.html). The model was constructed of 3.6-mm-cubic voxels; it was 177 cm tall and weighed 76 kg. Mason *et al* (2000) produced a very high spatial resolution model (voxel size 1 mm), classifying over 40 different tissue types, based on photographic male data from the VHP. The original data of the VHP were obtained from a 38-year-old male cadaver, 186 cm in height and 90 kg in weight (Xu *et al* 2000), while the voxel model weighs 105 kg due to the process of modelling. Xu *et al* (2000) also developed a model with the highest resolution based on photographic male data from the VHP, and named it 'VIP-man'. The model was segmented into about 1400 different structures with a resolution of $0.33 \times 0.33 \times 1$ mm^3; it was 186 cm tall and weighed 104 kg. VIP-man allows whole-body SAR estimation although such an estimation has not been reported.

The sizes of these models, except for the models developed using only the VHP, are close to the average body size of Caucasians (Western Europeans and North Americans), as described in the ICRP 23 or ICRP 66 (1994). On the other hand, body sizes and sizes of internal organs differ between Japanese and Caucasians (Tanaka 1988). It is not always

appropriate to use the above-described models to evaluate the SAR characteristics of Japanese subjects because the SAR is influenced by factors such as body size and position and size of internal organs. Saito *et al* (2001) developed a realistic whole-body voxel model of Japanese using x-ray computed tomography (CT) data of an adult male. The height and weight of this model were 170 cm and 65 kg, respectively, which are close to the height and weight of Japanese reference man (Tanaka 1988). However, the spatial resolution of the model is $0.98 \times 0.98 \times 10\,\mathrm{mm}^3$, which is comparable to the wavelength in human tissues at frequencies in the UHF or higher bands. As a result, the model cannot be used for numerical simulation at these frequencies.

In addition, all the adult models developed in the past were male models. No adult female model was developed, although some child female models (featuring relatively coarse spatial resolution) have been developed for ionizing radiation dosimetry (Zankl *et al* 1988). An adult female differs from an adult male in anatomical structure as well as in average body size. It is, therefore, strongly required to determine SAR characteristics in an adult female body and to distinguish these from those in males; naturally females will wear the same sorts of wireless devices.

The purpose of this study is to construct realistic high-resolution whole-body voxel models based on MRI data for Japanese adult males and females of average height and weight. The next section of this paper describes the acquisition of MRI data and the identification of tissues and organs for these models. These tissues and organs are then compared with those of Japanese reference man and other models (Dimbylow 1995, Gandhi and Furse 1995, Xu *et al* 2000). We then present basic SAR characteristics of these human models for the VHF/UHF bands. Finally, we discuss the anatomical structures and applications of these models.

2. Methods for constructing voxel models

In order to develop a whole-body voxel model, MR images are required for the entire body of the subject voxel model. The average height and weight of Japanese 18 to 30 years old are 171.4 cm and 63.3 kg for males and 159.1 cm and 52.6 kg for females (NIBH 1996). Based on the average data, candidate subjects for male and female models were recruited, and a male and female were chosen whose sizes were close to the Japanese average values. The male volunteer, 22 years old, was 172.8 cm tall and weighed 65.0 kg; the female volunteer, also 22 years old, was 160.0 cm tall and weighed 53.0 kg.

MR images of male and female subjects were acquired using an MRI device (Signa Hispeed LX; GE Medical Systems, Milwaukee, WI, USA) at Kitasato University Hospital. A complete set of axial images was acquired from the top of the head to the soles of the feet. Each image featured a slice thickness of 2 mm, and a matrix size of 256×256 with a 240 mm field-of-view (FOV) for the head and a 480 mm FOV for the body. Other scan parameters were optimized for the head and body separately in order to maximize contrast and to reduce data-acquisition time. The total time required for precise arrangement and image acquisition over the entire body for one subject was approximately 8 h. The subject was immobilized with a cast to restrict movement and to maintain the same position while being scanned, with feet and ankles positioned as if the subject were standing on the ground. The image acquisition was divided into several sessions in order to reduce the volunteer's stress. The cast enables good repeatability of the body location and position between each image acquisition session.

The transverse (axial) images of the whole body obtained by MRI scan were saved as 8-bit greyscale TIFF (tag image file format) images, which can be read and manipulated easily using a PC. The pixel size of the MR images (head area was $0.9375 \times 0.9375\,\mathrm{mm}^2$ and body

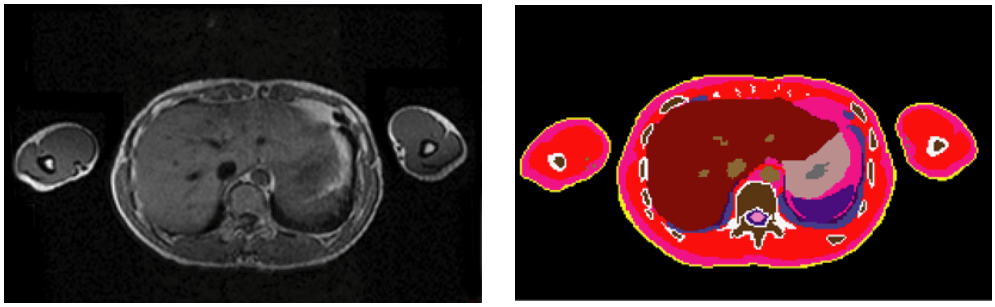

(a) (b)

Figure 1. An example of a transverse image before and after identification of tissues and organs. (a) Original MR image at abdomen level, (b) tissue- and organ-identified image at the same level.

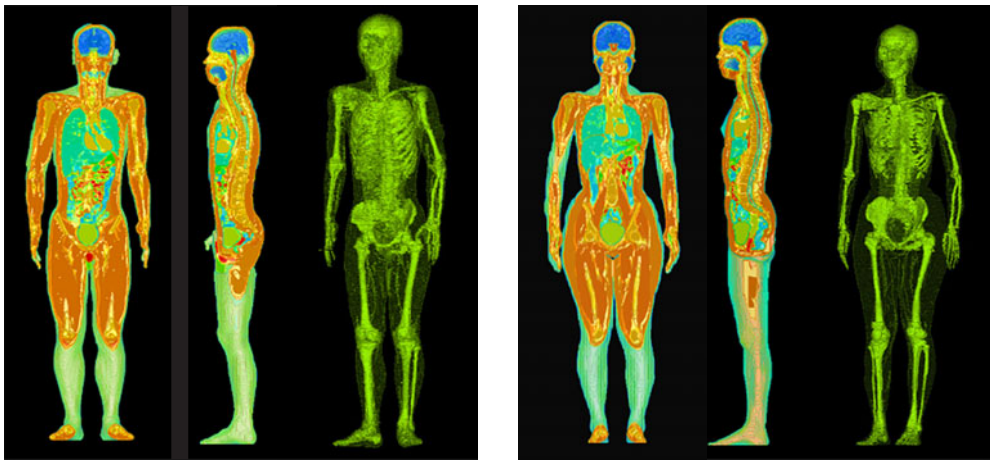

(a) (b)

Figure 2. Developed realistic voxel models for male and female. (a) Mid-coronal section display (left), mid-sagittal section display (middle) and bone enhanced image (right) for male. (b) Female model displayed similarly as the male model in (a).

area was 1.875×1.875 mm^2) was rescaled to 2×2 mm^2 to allow for a spatial resolution of $2 \times 2 \times 2$ mm^3 for the whole-body images. There were a total of 866 whole-body transverse images for the male and 804 for the female. These were used as original images to identify tissues and organs for each voxel.

It is impossible to divide the voxels in the original images into corresponding tissues or organs automatically with sufficient accuracy using presently available image-processing technologies. All tissue- and organ-identification processing was therefore performed individually by medical staff members using PC software. An example of an original image and an identified image is shown in figure 1. All identified transverse images were combined using our own developed software, and three-dimensional whole-body images were constructed. The boundaries of tissues and organs were not smooth in sagittal and coronal displays because the identification work by the staff was somewhat subjective. Therefore, the boundaries were smoothed by checking the three-dimensional images and the three orthogonal planes (axial, sagittal and coronal planes). Final positioning and shaping of the tissues and organs were performed under the supervision of medical doctors (radiologists) using three-dimensional

Table 1. Comparison of tissue and organ masses between the developed models and average Japanese adult male and female.

	Male			Female		
	Mass (g)			Mass (g)		
Tissue or organ	Model	Average[a] (Mean ± SD)	Model-to-average ratio	Model	Average[a] (Mean ± SD)	Model-to-average ratio
Brain	1399	1462.3 ± 111.5	0.96	1087	1323.5 ± 104.1	0.82
Heart	419	359.9 ± 87.7	1.16	239	266.7 ± 72.5	0.90
Liver	1185	1540.2 ± 307.5	0.77	1033	1275.2 ± 209.0	0.81
Pancreas	69.6	123.7 ± 31.9	0.56	42.0	102.2 ± 24.1	0.41
Spleen	146	140.2 ± 48.8	1.04	118	124.8 ± 51.2	0.95
Thyroid	15.2	18.87 ± 4.35	0.81	11.1	15.99 ± 4.88	0.70
Kidney	311	320	0.97	208	280	0.73
Small intenstine	335	590	0.57	326	450	0.72
Large intenstine	361	330	1.09	386	260	1.48
Stomach	193	140	1.38	107	110	0.97
Skeleton	11 186	8400	1.33	7668	6400	1.20
Fat	14 445	10 000	1.44	16 465	13 000	1.27
Muscle	26 566	25 000	1.06	15 689	20 000	0.78
Skin	3722	2400	1.55	2886	1800	1.60

[a] Data of Japanese reference man (Tanaka *et al* 1989) were used as reference for average Japanese values. However, data of Asian reference man (Tanaka and Kawamura 1996) were used for average values of tissues and organs without referring to Japanese reference man.

visualization software (INTAGE RV; Kubota Graphics Technologies, Inc., Tokyo, Japan). Consequently, the development of these models took over three years.

3. Anatomical details of the developed voxel models

Figure 2 shows the developed whole-body voxel models. These models are in the upright position, as if standing on the ground with the hands at the sides of body, are composed of voxels of $2 \times 2 \times 2$ mm^3, and are segmented into 51 different tissues and organs, in both the male and the female models. The masses of main tissues and organs of the developed models were compared with the average values for Japanese reference man (Tanaka *et al* 1989), while the masses of the tissues and organs not found in Japanese reference man were compared with those of Asian reference man (Tanaka and Kawamura 1996). The mass of each tissue and organ in the developed models was derived from the volume (the number of voxels) of each tissue and organ, combined with density values described for Asian reference man. These masses are listed in table 1. The masses of tissues and organs in the female model have a tendency to be lighter than average values of Japanese or Asian reference man. The masses of the large intestine, skeleton, fat and skin of both models were heavier than the average values. The masses of 60% of the identified tissues and organs in the male model were within ±30% of the average values. For the female model, on the other hand, the masses of 80% of the identified tissues and organs were within ±30% of the average values.

In table 2, the masses of the main tissues and organs of the developed male model are compared with those of NORMAN (Dimbylow 1995), Gandhi's model (Gandhi and Furse 1995) and VIP-man (Xu *et al* 2000). The mean ±SD of the ratios of the masses of the developed model to those of each of the other models were 0.88 ± 0.19 for NORMAN, 0.90 ± 0.19 for Gandhi's model and 0.89 ± 0.33 for VIP-man. In the developed model, 82%, 63% and 64% of tissues and organs were lighter than those of NORMAN, Gandhi's model

Table 2. Comparison of tissue and organ masses of male models.

	Tissue and organ masses (mass ratio of the developed model to other models) (g)			
Tissue or organ	Developed model	NORMAN[a]	Gandhi's model[b]	VIP-man[c]
Muscle	26 556	29 177 (0.91)	31 871 (0.83)	43 002.6 (0.62)
Body fat	14 445	–	14 873 (0.97)	–
Skeleton	11 186	10 177 (1.10)	9675 (1.16)	10 114.2 (1.11)
Skin	3722	4896 (0.76)	3329 (1.12)	2253.4 (1.65)
Brain	1399	1469[d] (0.95)	1673 (0.84)	1574[d] (0.89)
Liver	1185	1800 (0.66)	1759 (0.67)	1937.9 (0.61)
Stomach	193	212 (0.91)	–	159.5 (1.21)
Heart	419	340 (1.23)	–	398.7 (1.05)
Spleen	146	170 (0.86)	–	244 (0.60)
Kidney	311	318 (0.98)	304 (1.02)	335.4 (0.93)
Pancreas	69.6	104 (0.67)	114.8 (0.61)	82.9 (0.84)
Thyroid	15.2	26.4 (0.58)	–	27.6 (0.55)
Body weight	65 000	70 000 (0.93)	71 000 (0.92)	104 277 (0.62)

[a] Dimbylow (1995).
[b] Gandhi and Furse (1995).
[c] Xu *et al* (2000).
[d] Total mass of brain and nerves.

and VIP-man, respectively. Masses of the muscle, brain, liver and pancreas of the developed model were lighter than in the other models, while skeletal mass was greater than in the other models. In addition, it was also noted that the deviation of kidney mass among all models is small ($<10\%$).

4. Application to electromagnetic dosimetry

4.1. Method and models

The FDTD method was used to evaluate the internal electromagnetic fields of the human models exposed to E-polarized transverse electromagnetic (TEM) waves in the VHF/UHF bands propagating from the front to the back of the body. The incident power density was 1 mW cm^{-2}, which was the reference level for occupational exposure to EMFs at the VHF band (ICNIRP 1998). Second approximations of Mur's absorbing boundary conditions (Mur 1981) were assumed at all boundaries of the calculation region, such that the human models could be assumed to be in free space.

Errors due to artificial reflection from the calculation boundaries (truncation) are dependent on the distance between the boundaries and scattered bodies in the calculation region, as well as on the frequency of the simulated electromagnetic wave. Investigation revealed that the error due to boundaries set 80–160 cells apart from the nearest parts of the human models was evaluated to be not more than 0.5 dB for whole-body averaged SARs from 30 MHz to 3 GHz. Dimbylow (2002) also reported that the errors of E-field distribution in a 2 mm voxel sphere model were 2.3%, 6.6% and 9.8% at 900, 1800 and 3000 MHz, respectively, compared to Mie solutions, and that the errors of a 4 mm voxel sphere model were 2.1% and 2.5% at 100 and 35 MHz, respectively. Although Dimbylow (2002) used more effective boundary conditions (PML: perfect matched layer) than ours (Mur's second approximations), his report suggests that our calculation allows fairly quantitative discussion.

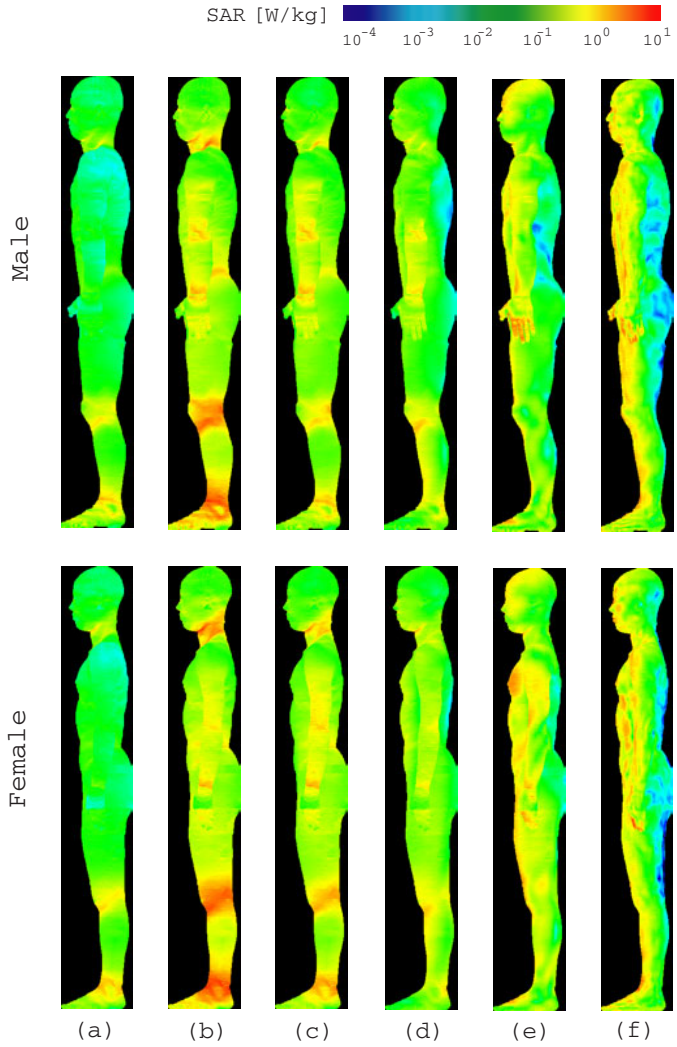

Figure 3. SAR distribution display on the surface of the male and female models exposed to E-polarized TEM waves: (a) 30 MHz, (b) 70 MHz, (c) 100 MHz, (d) 300 MHz, (e) 1 GHz and (f) 3 GHz.

In the calculation regions, electromagnetic properties corresponding to the tissues and organs were defined at each FDTD cell. The electrical properties (relative permittivity and conductivity) were taken from Gabriel (1996) and Gabriel *et al* (1996a, 1996b, 1996c). The electrical properties of tissues and organs not described in these sources were substituted with the electrical properties of other tissues described in these sources.

4.2. Results of electromagnetic dosimetry

SAR distributions on the surface of the male and female models are shown in figure 3. The SAR distributions of the vertical sections are also shown in figure 4. These figures indicate that the SAR distribution is strongly dependent on frequency but not on gender.

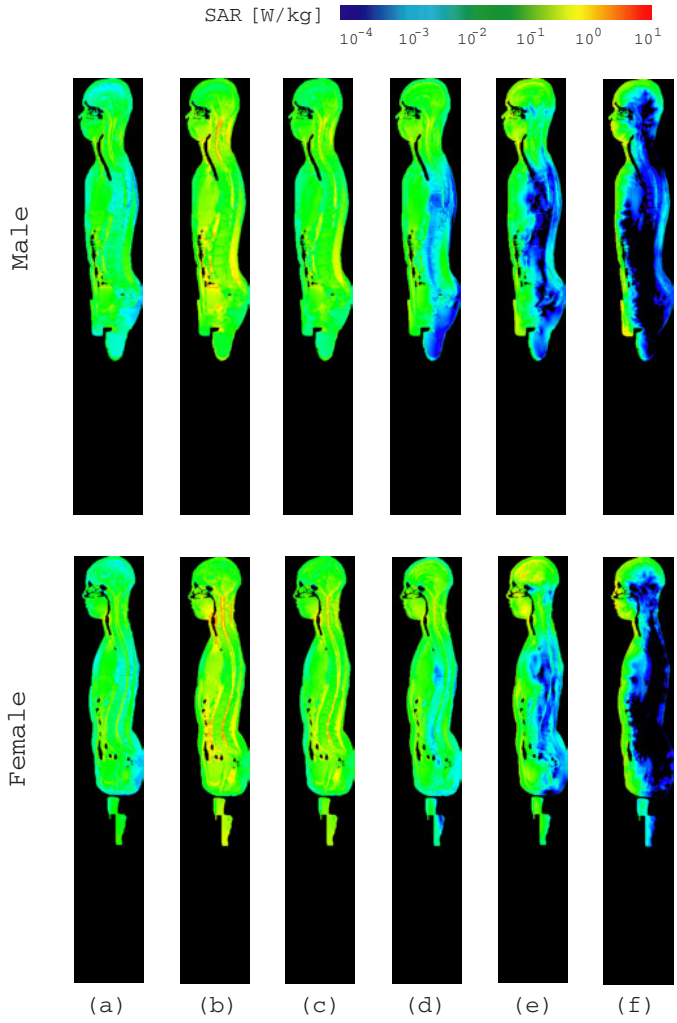

Figure 4. SAR distribution display in the mid-sagittal section of the male and female models. Exposure conditions are the same as those in figure 3.

The whole-body averaged SAR (WBA-SAR), which is used as the most important measure of thermal effects due to RF-EMF exposure, is shown in figure 5. The whole-body averaged SARs of multilayered prolate spheroidal models of an average male and female described in the Radiofrequency Radiation (RFR) Dosimetry Handbook (Durney *et al* 1986) and those of NORMAN (Dimbylow 1997) are also shown in figure 5. The long axes are 176 cm and 161 cm for the multilayered prolate spheroidal models of averaged male and female, respectively. The whole-body averaged SARs of all models become maximum around the whole-body resonant frequency (70 MHz) while Dimbylow (1997) reported that the whole-body resonance of NORMAN occurs at 65 MHz. It is shown that the differences in WBA-SARs between the male and female models are at most 1.1 dB. With respect to anatomy, gender does not affect WBA-SAR. Around the whole-body resonant frequency (70 and 100 MHz), good agreement is seen between our calculation and the RFR Dosimetry Handbook (Durney *et al* 1986), while significant difference is shown at the other frequencies. These results suggest that the RF

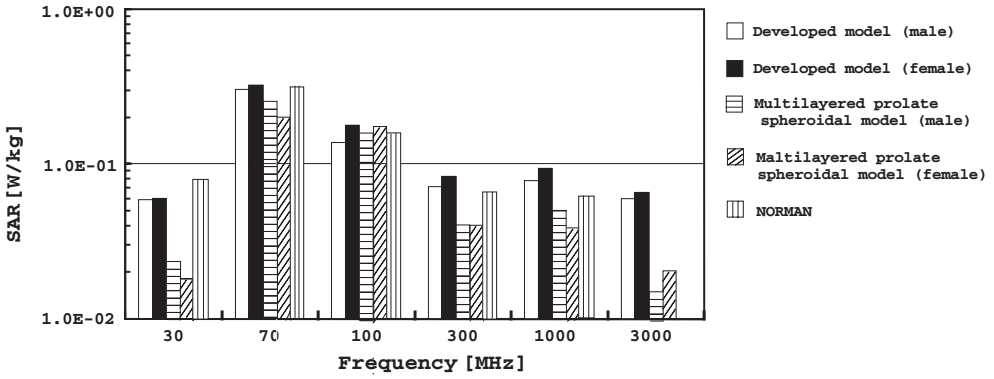

Figure 5. Whole-body averaged SARs (WBA-SARs) of the male and female models exposed to E-polarized TEM waves. The WBA-SARs are comparable to those of other models (Dimbylow 1997, Durney 1986). The result of NORMAN is not shown at 3 GHz.

power absorption depends on the tall length (long axis) around the whole-body frequency, while various factors can affect the SAR characteristics at other frequencies.

The maximum values of local SAR averaged over any one or ten grams of tissue—which are used as basic guidelines for localized exposure, such as the case of cellular-telephone use (ICNIRP 1998, IEEE 1999)—and the location of the maximum SARs are shown in figure 6. It is shown that at around the whole-body resonant frequency (70 MHz), the maximum local SARs become maximum and appear in the vicinity of the knee and ankle, which agrees with the results of Dimbylow's study (Dimbylow 1997). It is also shown that most of the maximum SARs occur in the extremities, with no significant difference found between the male and female models.

Tissue-averaged SARs are shown in figure 7. It is shown that the tissue-averaged SARs generally become maximum at around the whole-body resonance frequency (70 MHz). There is no consistent difference between the male and female results. SAR values averaged over male/female-inherent tissues are shown in figure 8. It is shown that the tissue-averaged SARs of the extruding organs, i.e., cavernous bodies (such as the penis), testes, and breast fat, can be higher than the WBA-SAR, while those of the other internal organs are less than or nearly equal to the WBA-SAR.

5. Discussion

In evaluating the impact of RF exposure, as described in the above section, the calculated SAR values averaged over the entire body, tissue, and any one or ten grams of tissue are used. The masses of tissues and organs are therefore an important factor. It is shown that most tissue and organ masses of the developed models were close to the average values of Japanese reference man or Asian reference man (table 1). However, several tissue and organ masses of the developed models differed considerably from average values. This is attributed in part to the deviation from the average values among the individual volunteers in terms of tissue and organ mass. Another reason for this difference is the spatial resolution, as described below.

The BMI (body mass index) values are 21.7 and 20.7 for the developed male and female models, respectively, which are in the normal range for Japanese adults. However, from table 1, the percentages of body fat were evaluated to be approximately 22% and 31% for the male and female models, respectively. These values slightly exceed the optimum range for Japanese adults. Despite our rigorous attention to detail in tissue and organ identification,

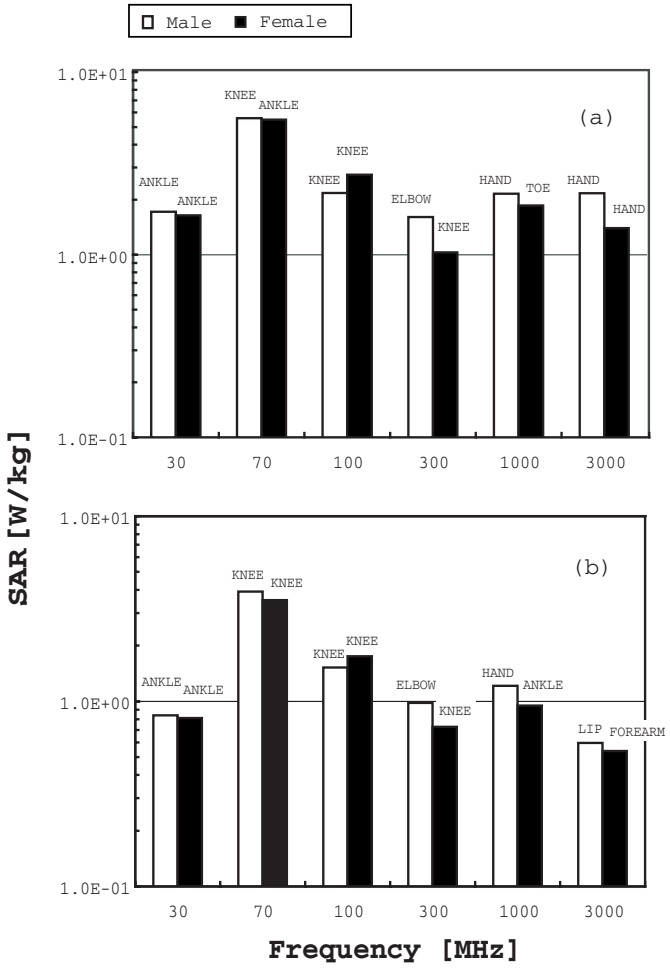

Figure 6. Maximum local SARs averaged over any 1 g mass of tissue (a) and 10 g mass of tissue (b) of the male and female models exposed to E-polarized TEM waves. The location of the maximum local SAR is described.

very small tissues (e.g., blood) and internal organs, surrounding visceral fat might be included in the percentage of body fat because of the limitation of voxel size and/or difficulty of tissue and organ identification in MR images. As a result, the percentage of body fat might be too high.

An important problem associated with voxel models is the overestimation of surface area, i.e., the masses of skin for the male and female models are heavier by 50% or more than the average value. These errors are caused by constructing the models with voxels of $2 \times 2 \times 2$ mm^3, while the actual thickness of skin is less than 2 mm in most parts. In addition, these errors are particularly marked for curved surfaces. The skin area of the developed male model is 16 918 cm^2 which is approximately the average value for Asian reference man (16 300 cm^2) (Tanaka and Kawamura 1996). Error in terms of skin mass would be considerably reduced by constructing a model with smaller voxels, as with VIP-man (Xu *et al* 2000).

The body weight and the tissue and organ masses of the developed male model are compared with those of Western male models (table 2). Our model differs greatly from

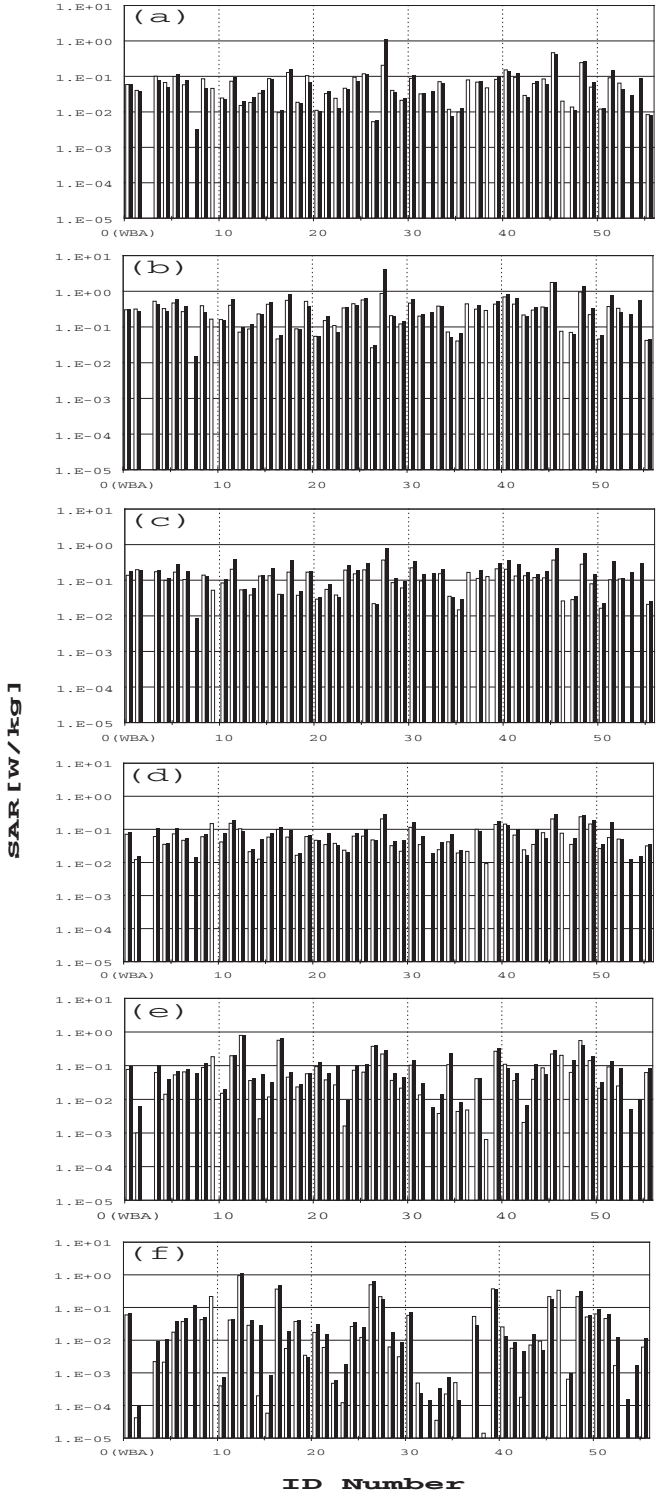

ID Number	Tissue and organ
0	WBA (Whole-body average)
1	Adrenals
2	Air (Internal)
3	Bile
4	Bladder
5	Blood
6	Bone marrow and cancellous bone
7	Breast fat [Female]
8	Cartilage
9	Cavernous body [Male]
10	Cerebellum
11	Cerebral spinal fluid
12	Cornea
13	Cortical bone
14	Diaphragm
15	Duodenum
16	Esophagus
17	Eye tissue (Sclera)
18	Fat
19	Gall bladder
20	Gray matter
21	Heart
22	Hypothalamus
23	Kidney
24	Large intestine
25	Large intestine contents
26	Lens
27	Ligament
28	Liver
29	Lung
30	Muscle
31	Nerve (Spinal cord)
32	Ovary [Female]
33	Pancreas
34	Pineal glands
35	Pituitary
36	Prostate [Male]
37	Salivary grand
38	Seminal vesicle [Male]
39	Skin
40	Small intestine
41	Small intestine contents
42	Spleen
43	Stomach
44	Stomach contents
45	Tendon
46	Testis [Male]
47	Thalamus
48	Thyroid
49	Tongue
50	Tooth
51	Trachea
52	Urine
53	Uterus [Female]
54	Vagina [Female]
55	White matter

Figure 7. Tissue-averaged SARs of the male and female models exposed to E-polarized TEM waves: (a) 30 MHz, (b) 70 MHz, (c) 100 MHz, (d) 300 MHz, (e) 1 GHz and (f) 3 GHz.

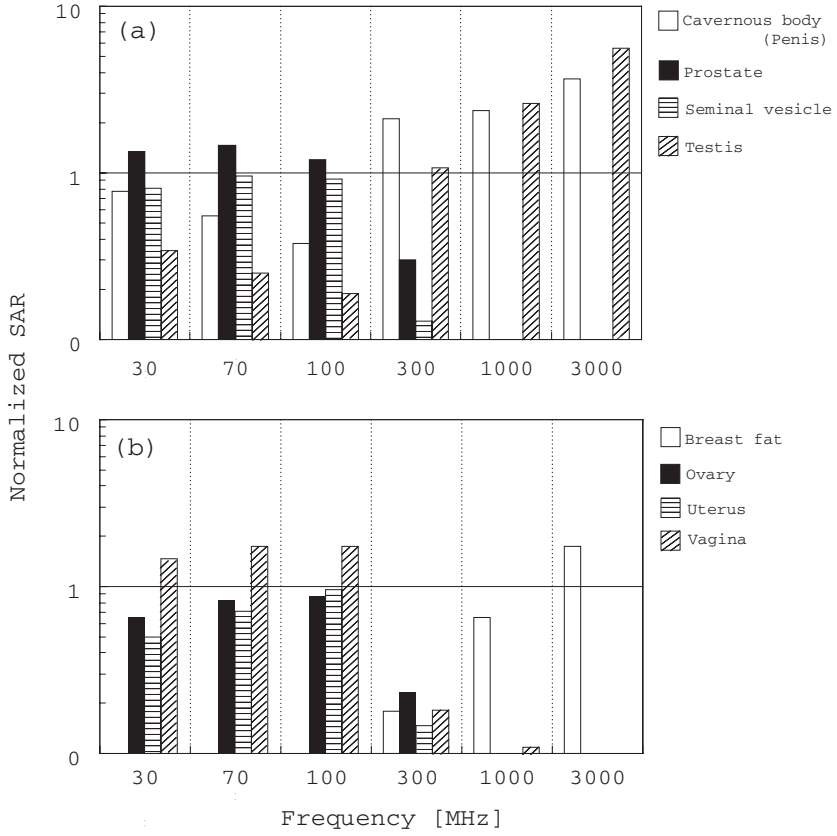

Figure 8. Inherent tissue SARs of male (a) and female (b). The SAR values are normalized by the whole-body averaged (WBA) SAR corresponding to that in figure 7.

Western models in weight (62–93%) and the masses of tissues and organs (55–165%). The masses of most tissues and organs in the developed model are lighter than those in Western models while the masses of some tissues and organs (skeleton, skin, heart and stomach) are heavier than those of VIP-man despite the subject being quite large (104 kg). As mentioned above, the limitation of voxel size can increase the volume of thin-structure/wall tissues and organs (skin, heart and stomach). The deviation of the skeletal mass may be attributed to individual variation. If Western models were to be scaled such that the total weight were equal to that of the average Japanese or Asian, masses of tissues and organs of those models will approach those of our development model. However, it appears to be very difficult to scale not only the figures but also the internal structures of the other models to coincide with those of average Japanese and Asian models. Our model is an optimal model for electromagnetic dosimetry for Asians, who account for about 58% (Tanaka *et al* 1989) of the world's population.

The developed models consist of 2 mm isotropic voxels. Because the upper limit of applicable frequency of the voxel model depends on the relationship between voxel size and wavelength (frequency), the developed models are the first whole-body models of average Japanese subjects that can be used for numerical simulation in the microwave region (up to 3 GHz). Furthermore, the female model is the first of its kind in the world. Therefore, the models enable the evaluation of SAR characteristics in the frequency band (800 MHz–2 GHz)

of cellular phones. These models are also used for evaluations in a higher frequency band (2.45 GHz) that may soon become widely used for wireless LAN (local area network) and other wireless communications. Moreover, these models can also be used for safety evaluations of novel portable communication terminals, i.e., wearable communication terminals positioned at various parts of the body.

The SAR characteristics inside a human body exposed to electromagnetic waves are influenced by the subject's shape and the masses and shapes of tissues and organs. In the future, Japanese models with average values of these characteristics will be required for various age groups. The developed whole-body voxel models will be applied not only for RF-safety evaluation but also for numerical simulation in various other research fields. Recently, for example, whole-body voxel models have been applied for precise estimation of the effect of ionizing radiation exposure on the human body (Zankl *et al* 1995, Jones 1995, 1998, Xu *et al* 2000, Chao *et al* 2001, Saito *et al* 2001), while mathematical models (Cristy 1980, Stewart *et al* 1993), in which the shape of a body as well as tissues and organs are defined by combinations of mathematical equations, have been widely used for the purposes of radiation protection, diagnosis and therapy. In addition, the developed models will contribute to elastic analysis in simulations of personal injury (e.g., in motor-vehicle collisions) and in thermal analysis under various environmental conditions, simply by replacing the electric constants applied to the tissues and organs of the voxel model with the elastic constant and the heat constant, respectively.

6. Conclusions

Realistic whole-body voxel models have been developed using MRI data from a Japanese adult male and female. The models consist of $2 \times 2 \times 2$ mm^3 voxels and are segmented into 51 different tissues and organs. Although some tissue and organ masses of the developed models deviate from average Japanese values due to limited spatial resolution, most of the masses are close to the average Japanese values. Therefore, highly precise simulation for Japanese subjects is possible using these whole-body voxel models. SAR evaluation for VHF/UHF bands has been demonstrated as an example of the application of these models (section 4). These models possess a high resolution of 2 mm, and enable electromagnetic exposure evaluation at high frequencies of up to 3 GHz. In addition, if parameters other than electric constants are applied to each tissue and organ of the models, the models may be used in a variety of research fields. We expect that the developed models will be used widely not only in the analysis of the electromagnetic field but also in a variety of research fields. We are planning to make data from the developed models widely available to the public for use in various research, after establishing the basic distribution conditions.

Acknowledgments

We are grateful to Professor Osamu Fujiwara of the Department of Electrical and Computer Engineering, Nagoya Institute of Technology. Parts of this work were supported by the vector supercomputer SX-6 (NEC) of the Communications Research Laboratory.

References

Chao T C, Bozkurt A and Xu X G 2001 Conversion coefficients based on the VIP-man anatomical model and EGS4-VLSI code for external monoenergetic photons from 10 keV–10 MeV *Health Phys.* **81** 163–83

Cristy M 1980 *Mathematical Phantoms Representing Children of Various Ages for Use in Estimates of Internal Dose* (Oak Ridge, TN: Oak Ridge National Laboratory) ORNL/NUREG/TM-367

Dawson T W, Caputa K and Stuchly M A 1997 A comparison of 60 Hz uniform magnetic and electric induction in the human body *Phys. Med. Biol.* **42** 2319–29

Dimbylow P J 1994 SAR calculations in an anatomically realistic model of a head for mobile communication transceivers at 900 MHz and 1.8 GHz *Phys. Med. Biol.* **39** 1537–53

Dimbylow P J 1995 The development of realistic voxel phantoms for electromagnetic field dosimetry *Proc. Int. Workshop on Voxel Phantom Development (6–7 July 1995)* (Chilton, UK: National Radiological Protection Board) pp 1–7

Dimbylow P J 1997 FDTD calculations of the whole-body averaged SAR in an anatomically realistic voxel model of the human body from 1 MHz to 1 GHz *Phys. Med. Biol.* **42** 479–90

Dimbylow P J 2002 Fine resolution calculation of SAR in the human body for frequencies up to 3 GHz *Phys. Med. Biol.* **47** 2835–46

Durney C H, Massoudi H and Iskander M F 1986 *Radiofrequency Radiation Dosimetry Handbook* 4th edn (Brooks Air Force Base, TX: USAF School of Aerospace Medicine) USAFSAM-TR-85–73

Gabriel C 1996 Compilation of the dielectric properties of body tissues at RF and microwave frequencies *Armstrong Laboratory, Brooks Air Force Base, Tech. Rep.* AL/OE-TR-1996–0037

Gabriel C, Gabriel S and Corthout E 1996a The dielectric properties of biological tissues: I. Literature survey *Phys. Med. Biol.* **41** 2231–49

Gabriel S, Lau R W and Gabriel C 1996b The dielectric properties of biological tissues: II. Measurements in the frequency range 10 Hz to 20 GHz *Phys. Med. Biol.* **41** 2251–69

Gabriel S, Lau R W and Gabriel C 1996c The dielectric properties of biological tissues: III. Parametric models for the dielectric spectrum of tissues *Phys. Med. Biol.* **41** 2271–93

Gandhi O P 1987 The ANSI radiofrequency safety standard: its rational and some problems *IEEE Eng. Med. Biol. Mag.* 22–5

Gandhi O P and Furse C M 1995 Millimeter-resolution MRI-based models of the human body for electromagnetic dosimetry from ELF to microwave frequencies *Proc. Int. Workshop on Voxel Phantom Development (6–7 July 1995)* (Chilton, UK: National Radiological Protection Board) pp 24–31

Gandhi O P, Lazzi G and Furse C M 1996 Electromagnetic absorption in the human head and neck for mobile telephones at 835 and 1,900 MHz *IEEE Trans. Microwave Theory Tech.* **44** 1884–97

ICNIRP 1998 Guidelines for limiting exposure to time-varying electric, magnetic, and electromagnetic fields (up to 300 GHz) *Health Phys.* **74** 494–522

ICRP 1975 Report of the Task Group on Reference Man *ICRP Publication 23*

ICRP 1994 Human Respiratory Tract Model for Radiological Protection *ICRP Publication 66*

IEEE 1999 *IEEE Std C95.1–1999; IEEE Standard for Safety Levels with Respect to Human Exposure to Radio Frequency Electromagnetic Fields, 3 kHz to 300 GHz*

Jones D G 1995 Use of voxel phantoms in organ dose calculations *Proc. Int. Workshop on Voxel Phantom Development (6–7 July 1995)* (Chilton, UK: National Radiological Protection Board) pp 90–7

Jones D G 1998 A realistic anthropomorphic phantom for calculating specific absorbed fractions of energy deposited from internal gamma emitters *Radiat. Prot. Dosim.* **79** 411–4

Mason P A, Ziriax J M, Hurt W D, Walter T J, Ryan K L, Nelson D A, Smith K I and D'Andrea J A 2000 Recent advancements in dosimetry measurements and modeling *Radio Frequency Radiation Dosimetry* ed B J Klauenberg and D Miklavcic (Dordrecht: Kluwer) pp 141–55

Mur G 1981 Absorbing boundary conditions for the finite-difference approximation of the time domain electromagnetic field equations *IEEE Trans. Electromag. Compat.* **23** 377–82

NIBH 1996 *Human Body Dimensions Data for Ergonomic Design* (Tokyo: Research Institute of Human Engineering for Quality Life)

Okoniewski M and Stuchly M A 1996 A study of the handset antenna and human body interaction *IEEE Trans. Microwave. Theory Tech.* **44** 1855–64

Saito K, Wittmann A, Koga S, Ida Y, Kamei T, Funabiki J and Zankl M 2001 Construction of a computed tomographic phantom for a Japanese male adult and dose calculation system *Radiat. Environ. Biophys.* **40** 69–76

Stewart R D, Tanner J E and Leonowich J A 1993 An extended tabulation of effective dose equivalent from neutrons incident on a male anthropomorphic phantom *Health Phys.* **65** 405–13

Tanaka G 1988 Japanese reference man 1988–III. Masses of organs and tissues and other physical properties *Nippon Acta Radiol.* **48** 509–13

Tanaka G and Kawamura H 1996 *Anatomical and Physiological Characteristics for Asian Reference Man—Male and Female of Different Ages: Tanaka Model* (Hitachinaka: National Institute of Radiological Sciences) NIRS-M-115

Tanaka G, Nakahara Y and Nakajima Y 1989 Japanese reference man 1988–IV. Studies on the weight and size of internal organs of normal Japanese *Nippon Acta Radiol.* **49** 344–64

Wang J and Fujiwara O 2000 FDTD analysis of dosimetry in human head model for a helical antenna portable telephone *IEICE Trans. Commun.* E **83-B** 549–54

Watanabe S, Taki M, Nojima T and Fujiwara O 1996 Characteristics of the SAR distributions in a head exposed to electromagnetic fields radiated by a hand-held portable radio *IEEE Trans. Microwave Theory Tech.* **44** 1874–83

Xu X G, Chao T C and Bozkurt A 2000 VIP-man: an image-based whole-body adult male model constructed from color photographs of the Visible Human Project for multi-particle Monte Carlo calculations *Health Phys.* **78** 476–86

Zankl M, Petoussi-Henss N and Wittmann A 1995 The GSF voxel phantoms and their application in radiology and radiation protection *Proc. Int. Workshop on Voxel Phantom Development (6–7 July 1995)* (Chilton, UK: National Radiological Protection Board) pp 98–104

Zankl M, Veit R, Williams G, Schneider K, Fendel H, Petoussi N and Drexler G 1988 The construction of computer tomographic phantoms and their application in radiology and radiation protection *Radiat. Environ. Biophys.* **27** 153–64

Zubal I G, Harrell C R, Smith E O and Smith A L 1995 Two dedicated software, voxel-based, anthropomorphic (torso and head) phantoms *Proc. Int. Workshop on Voxel Phantom Development (6–7 July 1995)* (Chilton, UK: National Radiological Protection Board) pp 105–11